



Characterization of the interface of two dental palladium alloys cast on a prefabricated implant gold cylinder

Vasilis K. Vergos, Triantafillos D. Papadopoulos*

Department of Biomaterials, Dental School, National and Kapodistrian University of Athens, Thivon 2 115 27, Athens, Greece

ARTICLE INFO

Article history:

Received 4 August 2008

Received in revised form 1 December 2008

Accepted 13 December 2008

Available online 24 December 2008

Keywords:

Dental alloys

Microstructure

Corrosion

Metallography

Scanning electron microscopy (SEM)

ABSTRACT

The interface between two dental alloys (Pd–Cu–Ga, Pd–Ga) cast to a prefabricated gold cylinder in two thicknesses (1, 2 mm) was investigated. Specimens were observed in optical and scanning electron microscopes. Line scan microanalysis by EDS was performed and polarization curves were taken. Gold cylinders shape was preserved. Characteristic elongated grains were detected at the gold cylinder alloy. The boundaries between the cylinder and the cast-to alloys were distinct. The 2 mm thick Pd–Ga alloy cast to the gold cylinder revealed high porosity at the interface, while the rest of the subgroups showed no or negligible porosity. Line scan analysis revealed the gradual diffusion of the main elements of each alloy in the structure of the gold cylinder and vice-versa in a 3–5 μm zone. Corrosion behaviour was estimated by cyclic polarization tests in 1 M lactic acid. The polarization curves showed negative hysteresis. In the reverse anodic scan the current density was less than that for the forward scan. This fact confirms that all the tested materials are not susceptible to corrosion in 1 M lactic acid.

© 2008 Elsevier B.V. All rights reserved.

1. Introduction

In order to fabricate the prosthetic superstructures on osseointegrated dental implants an alloy (*cast-to alloy*) is cast on a prefabricated implant gold cylinder (*gold cylinder*). In this technique the machined wrought structure of the gold cylinder is incorporated in the cast framework, providing precise fitting of the prosthetic superstructure on the implant fixtures. Additionally, precise fitting, gold cylinders offer better mechanical properties to the prosthetic superstructures [1].

To achieve a complete incorporation between the wrought microstructure of the gold cylinder and the cast-to alloy, it is critical to avoid microstructural changes during laboratory procedures. A crucial factor is the alloy casting temperature, which must be 80–100 °C lower than gold cylinder's melting temperature [2,3]. Strict evidences of a successful union between the two alloys (cast-to and gold alloy) are preservation of the wrought gold alloy microstructure, controlled elemental diffusion, absence of porosity in the alloy mass and their interface, lack of interfacial reaction regions and well-defined boundaries between cast-to alloy and gold cylinder [4,5].

In the early 1980s high-palladium alloys were introduced in the dental field as an alternative to gold alloys for the fabrication of implant superstructures [6,7]. Alloys containing more than 75%wt palladium are cost-effective and possess good mechanical

properties. Two types are available: The Pd–Cu–Ga alloy (1st generation) and the Pd–Ga alloy (2nd generation). They also contain other elements (Au, Pt, Ag, Sn, Ir, In, Ru) in lower concentrations. Because of their complex microstructures, these alloys are more technique sensitive [8,9]. The Pd–Cu–Ga alloy exhibits well-defined grain structure, which contains eutectic or lamellar dendritic constituents. The Pd–Ga alloy exhibits grains with a Pd-rich matrix boundary with fine scale precipitates, without eutectic reaction regions. Despite the absence of Cu, which is responsible for their lower mechanical properties, these alloys are acceptable for clinical use. [10,11]

It has been reported in the literature that thick castings have different microstructure compared to thin castings of the same alloy system [8]. The amounts of eutectic constituents in Pd–Cu–Ga are greater in thin sections or in near-surface portions of a casting. This has been attributed to the different rate of heat flow during solidification between the casting and the much cooler investment [8]. It is known that changes in microstructure lead to changes of mechanical and chemical properties [1,5]. A well documented microstructural change is due to the high affinity between Pd and C contained in some dental investments and crucibles. [12,13]. This interaction between microstructure and different thicknesses of implant superstructures has not been clarified. It would be interesting to investigate possible effects of the use of various cast-to alloys types of different thickness.

Many researchers have underlined the negative effect of corrosion on the clinical performance of the prosthetic superstructures of osseointegrated dental implants. [14,15]. Especially palladium ion release because of corrosion may be related to biocompatibility,

* Corresponding author. Tel.: +302107461100; fax: +302107461306.

E-mail address: trpapad@dent.uoa.gr (T.D. Papadopoulos).

Table 1
Materials tested.

Commercial name	Type of alloy	Manufacturer	Batch no.
Mentor P	Pd–Cu–Ga	Elementdental (Hagen, Germany)	04060713
IPSD.SIGN84	Pd–Ga	Ivoclar–Vivadent, (Schaan, Liechtenstein)	1018304
IPSD.SIGN98	Au–Pt	Ivoclar–Vivadent, (Schaan, Liechtenstein)	109287
MW-GPC10	Gold implant cylinder	MIS, (Shlomi, Israel)	40513

Table 2
Composition of the cast-to alloys and the prefabricated gold cylinder (wt%).

Elements	MW-GPC10	MENTOR P	IPS d.SIGN84	IPS d.SIGN98
Gold	60.0	1.4	9.0	85.9
Platinum	19.0	–	–	12.1
Silver	–	–	3.0	–
Palladium	20.0	78.5	75.2	–
Copper	–	11.5	–	–
Tin	–	–	–	1.5
Iridium	Balanced	0.2	–	–
Indium	–	–	6.5	<1.0
Gallium	–	8.5	6.0	–
Ruthenium	–	–	<1.0	–

while composition and structure influence the corrosion resistance of these alloys. In a Pd–Ga alloy increased surface oxidation was observed [16].

The aim of the present study was to characterize the interface between two cast alloys (Pd–Cu–Ga, Pd–Ga) in combination with a prefabricated gold cylinder, when two different cast thicknesses were used, as well as to examine the corrosion behavior of the different interfaces.

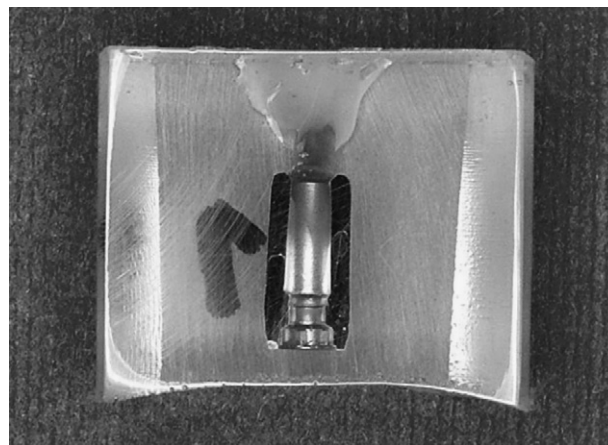
The Null hypothesis of the study was that the thickness and/or the type of the cast alloy do not affect the quality of the union between the prefabricated wrought gold cylinder and the cast-to alloy. High corrosion resistance is not expected for all the examined combinations.

2. Materials and methods

Two high-palladium dental alloys, one Pd–Cu–Ga (Mentor P) and the other Pd–Ga alloy (IPSD.SIGN84), were selected as cast-to alloys. A high-gold alloy (IPSD.SIGN98) was also used as control. These alloys were cast-to on the same type of a prefabricated gold implant cylinder (MW-GPC10) (Table 1). Alloy compositions and properties are presented in Tables 2 and 3.

Twelve specimens were produced and divided in three equal groups. In group A the ternary system Pd–Cu–Ga was cast-to to the gold cylinder, whereas the binary system Pd–Ga was cast-to to the gold cylinder in group B. The high gold alloy was cast-to to the gold cylinder in group C (control group). In two of the specimens of every group the thickness of the cast-to alloy was 1 mm (subgroups A1, B1 and C1), while the alloy thickness of the other two specimens was 2 mm (subgroups A2, B2 and C2) (Table 4).

For the fabrication of the specimens 12 gold cylinders were waxed using an appropriate hard inlay casting wax (Inlay Wax, Whip Mix Corp, Ky, USA) peripherally, following a stable and reproducible way. Half of them were waxed to a thickness of 1 mm and the other half to a thickness of 2 mm. Waxed gold cylinders were sprued

**Fig. 1.** Specimen prepared for optical and scanning electron microscopy.

and invested in a carbon-free phosphate-bonded investment material (Bellavest T, Bego BGW&Co, Bremen, Germany). Casting followed the manufacturer's instructions, by melting the alloys in individual ceramic crucibles, using a multiorifice gas-oxygen torch and a standard broken-arm centrifugal casting machine (Minigraft, Ugin, Seyssins, France). Each of the three types of alloys mentioned above was used for the production of four castings.

The castings were divested, air-abraded with aluminum oxide particles (50 μm) and embedded in transparent auto-polymerizing epoxy resin (Durafix-2, Struers, Copenhagen, Denmark). After resin polymerization the specimens were sectioned with a diamond disk at low speed under water-cooling, using a microtome (Macrotope 2, Metals Research, Cambridge, UK). Sectioning was performed in a direction parallel to the long axis of the gold cylinder (Fig. 1), followed by grinding with SiC papers under continuous water-cooling up to 2000 grit and polishing with 0.01 μm alumina powders in a grinding-polishing machine (ECOMET III, Buehler, Evanston, Ill, USA). The specimens were then cleaned for 10 min in an ultrasonic-bath (Vitasonic II, Vita Zahnfabrik, Bad Sackigen, Germany), using an 70% aqueous ethanol solution and air-dried.

Half of the sectioned specimens were observed in an optical microscope (Eclipse 200, Nikon, Kogaku, Japan) at 10 \times and 20 \times magnifications. To reveal the as-cast microstructures, specimens were chemically etched in aqua regia solutions (hydrochloric and nitric acids). Etching times and solution concentrations were adjusted properly for each alloy. The preservation of the cylinder shape, the maintenance of the alloy microstructure, the existence of distinct boundaries between alloys, the absence of oxide layer formation and the possible presence of pores within the interfaces were evaluated.

The other half of the specimens were observed in a scanning electron microscope (Quanta 200, FEI, Hillsboro, Oregon, USA). Line scans, in standard lines across the interface cylinder–cast alloy were received to study changes of element

Table 3
Properties of used alloys.

	MW-GPC10	Mentor P	IPS d.SIGN84	IPS d.SIGN98
Density (g/cm^3)	–	10.9	11.3	18.9
Vickers hardness	145	240	295	220
Modulus of elasticity (MPa)	–	–	117000	80000
Melting range ($^{\circ}\text{C}$)	1400–1490	1090–1165	1140–1335	1055–1170
Casting temperature ($^{\circ}\text{C}$)	–	1400	1390–1450	1225–1285

Table 4
Classification of groups and subgroups.

Group A Pd–Cu–Ga cast-to alloy on gold cylinder		Group B Pd–Ga cast-to alloy on gold cylinder		Group C Au–Pt cast-to alloy on gold cylinder (control group)	
Subgroup A1 (1 mm) $n=2$	Subgroup A2 (2 mm) $n=2$	Subgroup B1 (1 mm) $n=2$	Subgroup B2 (2 mm) $n=2$	Subgroup C1 (1 mm) $n=2$	Subgroup C2 (2 mm) $n=2$

concentrations and possible abrupt diffusion of elements. Microanalysis was made by an Energy-Dispersive X-Ray Spectrometer (EDS, CDU, Sapphire EDAX Int, Mawhaw, NJ, USA) with an extra thin beryllium window on secondary electron images (SEI) in high magnifications. Quantitative non standard analysis with ZAF-correction

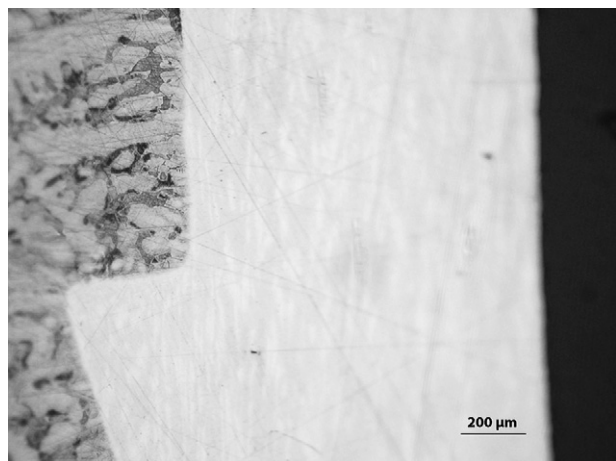


Fig. 2. Cross-section of a 1 mm Pd–Cu–Ga cast-to the gold cylinder specimen (subgroup A1) in magnification 10× in optical microscope. A close contact without pores and voids between the two materials was obtained.

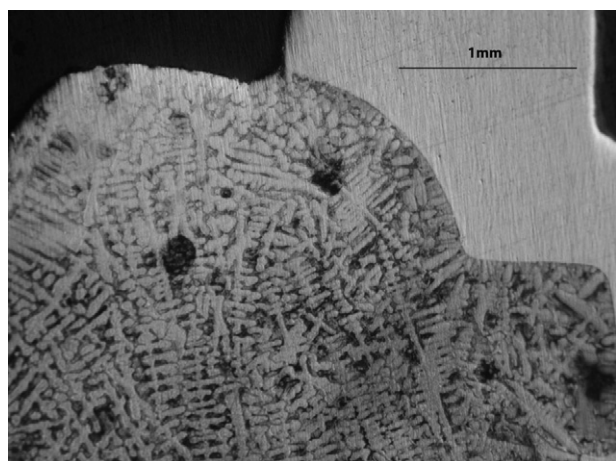


Fig. 3. Cross-section of a 2 mm Pd–Cu–Ga cast-to the gold cylinder specimen (subgroup A2) in magnification 10× in optical microscope. A close contact without pores and voids between the two alloys was obtained.

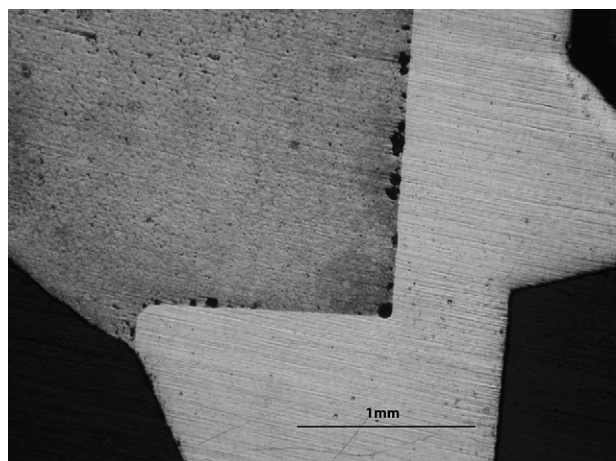


Fig. 4. Cross-section of a 2 mm Pd–Ga cast-to the gold cylinder specimen (subgroup B2) in magnification 10× in optical microscope. Extensive porosity between the two alloys was revealed.

method was applied. The elements studied were palladium, gallium, gold, platinum, silver, copper, tin, iridium, indium and ruthenium.

One representative specimen of every subgroup was prepared for corrosion tests. The specimens were ground until the sprue of the casting was revealed in purpose to make them conductive. Then the upper surface, including the two alloys and their interface, was polished with SiC papers up to 1000 grit, cleaned for 10 min in an ultrasonic bath with distilled water and left to dry. Cyclic polarization measurements were made with a potentiostat (Versa Stat II, EG&G Instruments, Princeton, TN, USA) to evaluate the corrosion behaviour of the tested alloys. The apparatus and the polarization cell conformed to ASTM G5-94 standards. An Ag–AgCl electrode was used as a reference and the platinum plate as an auxiliary counter electrode. A solution of 1 M lactic acid was the irrigating solution, which was heated to 37 °C until the end of the tests. Then, the specimens were placed in the polarization cell for 1 h before initiating polarization. Polarization curves were obtained with a potential scan rate of 5 mV/min.

3. Results

The interface quality observed in the optical microscope revealed that the shape of all the specimens was preserved. Moreover, characteristic microstructure with elongated grains along the longitudinal axis was detected at the cylinder alloy (Fig. 2). The interfaces between the cylinder and the cast-to alloys were distinct in all specimens (Fig. 3). The specimens of subgroup B2 (2 mm thick Pd–Ga alloy cast-to on the gold cylinder) revealed high porosity at the interface, while the rest of the subgroups showed

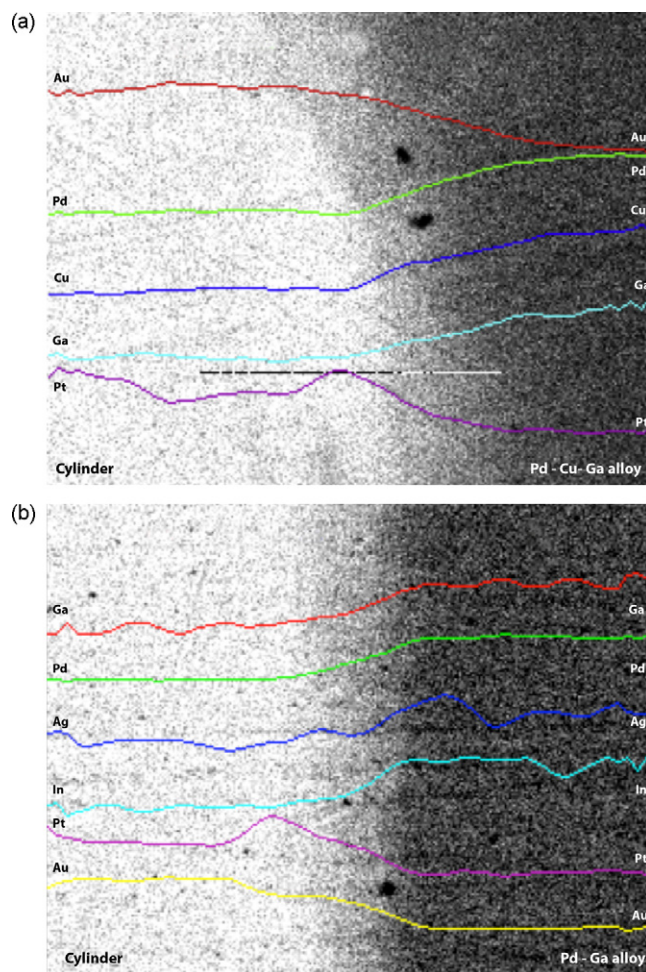


Fig. 5. (a) Line scan image of a 2 mm Pd–Cu–Ga cast-to the gold cylinder specimen (subgroup A2). A gradual decrease of the concentrations of elements is revealed within a 3–4 μm diffusion zone. Randomly located solely medium size pores are present and (b) line scan image of a 2 mm Pd–Ga cast-to the gold cylinder specimen (subgroup B2). A gradual decrease of the concentrations of elements is revealed within a δ about 4 μm diffusion zone. Medium size pores are present, accompanied by small-sized pores spread all over the diffusion zone.

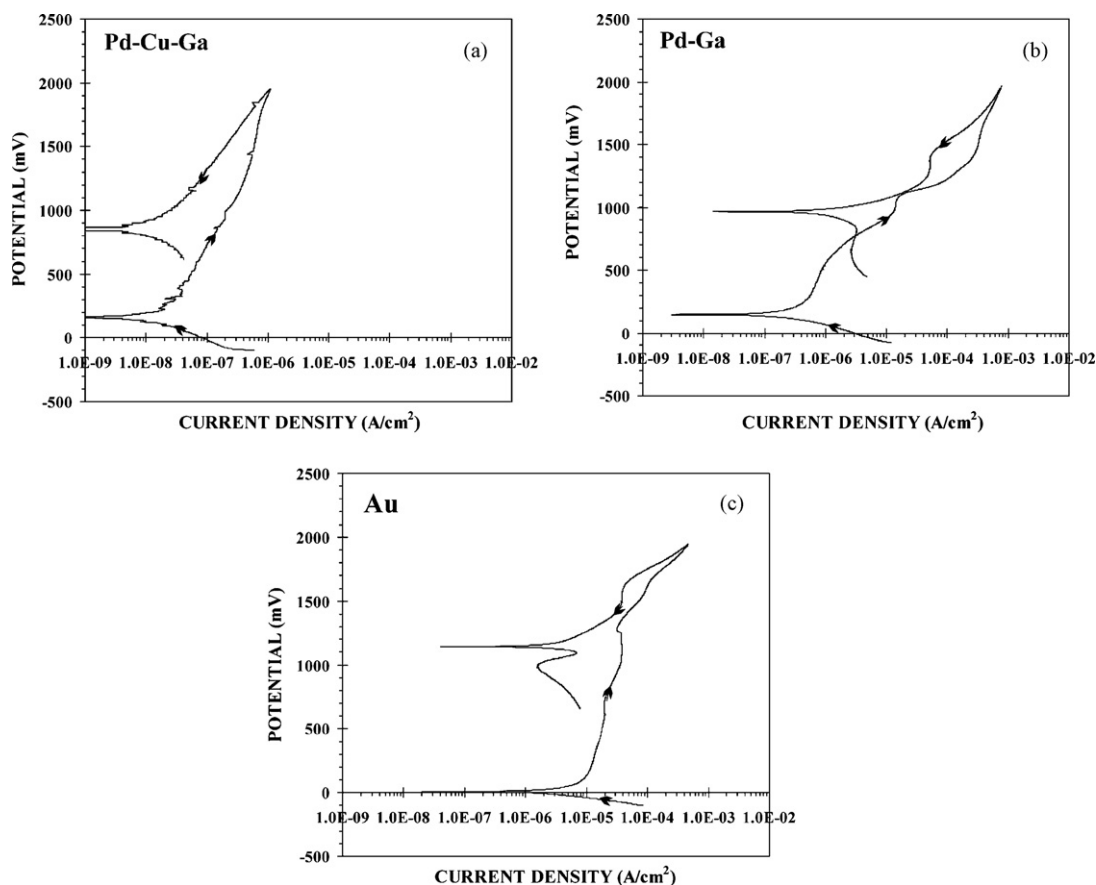


Fig. 6. (a), (b), (c) Typical cyclic polarization curves from a Pd–Cu–Ga (a), Pd–Ga (b) and a gold alloy (c) specimens immersed in 1 M lactic acid. It can be observed that all the polarization curves showed negative hysteresis, as in the reverse anodic scan the current density was less than that for the forward scan.

negligible porosity (Fig. 4). SEM images revealed randomly located solely medium pores for group A, while spread porosity across the diffusion zone was consisted of minor and medium size pores in specimens of group B.

The line scans revealed the gradual diffusion of the main elements of each alloy in the structure of the gold cylinder and vice-versa, verifying the close contact between the two alloys. More specifically, in the case of specimens of group A a gradual decrease of the concentrations of elements Au and Pt from the cylinder to the cast-to alloy and a gradual decrease of the concentrations of the elements Pd, Ga and Cu from the cast alloy to the cylinder was recorded, independently of thickness. The width of the diffusion zone was estimated to be 3–4 μm . A remarkable observation was the increased concentration of Pt immediately under the diffusion zone. In the case of specimens of group B a decrease in the concentrations of the elements Au and Pt was observed from the cylinder to the cast-to alloy and an gradual decrease of the concentrations of the elements Pd, Ga, In and Ag from the cast alloy to the cylinder (Fig. 5a). The diffusion zone was estimated to be about 4 μm . The Pt concentration was increased immediately under the diffusion zone from the site of the cylinder and the same increased concentration was detected for Ag from the site of the cast alloy. In specimens of subgroup B2, the elemental transition from one direction to the other was abrupt with changes in the concentration of the tested elements within the mass of the alloys near the interface (Fig. 5b). All the other combinations did not reveal any difference within the interface zone, independently of the type of alloy and/or the casting thickness.

Cyclic polarization results are presented in Fig. 6a–c. It can be observed that all the polarization curves showed negative hysteresis, as in the reverse anodic scan the current density was less

than that for the forward scan. The corrosion potential values E_{corr} for the Pd–Cu–Ga alloy ($E_{\text{corr}} = 158 \text{ mV}$) and for the Pd–Ga alloy ($E_{\text{corr}} = 154 \text{ mV}$) were similar, while the corrosion potential for the Au alloy ($E_{\text{corr}} = 7 \text{ mV}$) was much lower. Also, the current densities of the alloys Pd–Cu–Ga, Pd–Ga and Au were of the order of 10^{-9} , 10^{-8} and 10^{-7} A/cm^2 , respectively.

4. Discussion

According to the results of the present study, the hypothesis was verified because all groups presented an acceptable behavior, independently of the type of the alloy or the thickness of the specimens used. The hypothesis was not verified only for subgroup B2 (2 mm thick Pd–Ga alloy cast-to on the gold cylinder). Concerning corrosion resistance, the hypothesis was not verified because all examined combinations presented high corrosion resistance.

Carr and Brantley [5] recorded an acceptable metal to metal union with maintenance of cylinder microstructure up to the interface, absence of interfacial reaction regions and lack of porosity created by volatilization of components from Pd alloys during the casting process. Based on the cast interface criteria as proposed by Carr and Brantley [4], the preservation of the cylinder shape, the maintenance of the alloy microstructure, the existence of distinct boundaries between alloys and the possible formation of pores within the interfaces were also recorded in the present study. The extended voids present in subgroup B2 specimens can be attributed to the poor castability of the Pd–Ga binary alloy in combination with the lower heat flow due to the higher thickness of the specimen (2 mm). Carr and Brantley [8] have already reported that the rate of heat flow from the solidifying alloy into the cool investment may play an important role in the microstructure quality of the castings.

Indeed the higher melting temperature of Pd–Ga alloy compared to the other cast-to alloys used, created a higher temperature difference between the solidifying castings and the much cooler investment material. Gilson et al. [17] had early (1965) observed the negative influence of the increasing thickness of the castings in the quality of the union of different dental alloys. This might lead to inferior clinical performance of the implant superstructure.

In the present study the line scan analysis revealed gradual elemental concentrations from the bulky mass of the gold cylinder to the bulky mass of the cast-to alloy for both Pd alloys. Diffusion of multiphase alloy systems is complex. It is affected from the lattice type, the melting point of the participating elements and their atomic radius. Better diffusion is observed in the case of same lattice type, while atoms with a lower melting point and similar atomic radius possess a higher diffusion coefficient (D) [18]. In the present study the atomic radius of the participating elements are similar (about 4 Å) and their lattice type is face centered cubic (fcc). Ga possesses a low melting point of 296 °C resulting in a better diffusion.

In an elemental spot analysis [5] in seven regions across the interface between the bulk of a gold cylinder (SGC 30) to the bulk of a cast-to Pd–Ga alloy (IS 85), at a total distance of 40 μm, it was found that Ga diffused approximately 14 μm across the interface from the alloy into the cylinder and Pt diffused similarly from the cylinder into the cast alloy. Also in another study [4] the interdiffusion of Au and Pd over an approximately 20 μm region across the interface between a gold cylinder (DCA 072) and a Pd–Ga alloy (IS 85) exhibited metal to metal bonding. The concentrations of Au and Pd appeared to decrease more gradually over a distance of approximately 10 μm at the interface between the cast-to alloy and the cylinder. The authors reported no apparent differences in the microstructures of thick versus thin sections of castings alloys.

According to the results of the present study, the cyclic polarization curves exhibit negative hysteresis, given that in the reverse anodic scan the current density is lower than that for the forward scan. This fact confirms that all the tested materials are not susceptible to corrosion in 1 M lactic acid. Moreover, although a passive region is observed in the polarization curves concerning the Pd–Ga and Au alloys, a passive region is not present for the Pd–Cu–Ga alloy, as the potential continuously increases following current increase. This fact is probably due to the presence of copper, which deteriorates the corrosion behaviour [19].

5. Conclusions

Under the limitations of the present study the following conclusions can be derived:

There is no significant influence of the type of the cast-to alloys on the cylinder shape, the alloy microstructure, the existence of distinct boundaries between alloys, the absence of oxide layer formation and the presence of pores within the interfaces.

Also the thickness of the cast-to made alloys did not influence significantly the above parameters. The only exception was for the 2 mm thickness Pd–Ga alloy which revealed high porosity at the interface and abrupt elemental transition.

The alloys Pd–Cu–Ga, Pd–Ga and Au are not susceptible to corrosion in 1 M lactic acid.

Acknowledgements

We thank MIS Company for supporting part of the project and Metallurgists Mrs Darabara M. and Spiros Zinelis for helping us in metallurgical analysis and corrosion tests, respectively.

References

- [1] G.E. Dieter, *Mechanical Metallurgy*, McGraw-Hill Book Co., London, 1988.
- [2] G.C. Craig, *Restorative Dental Materials*, eighth ed., Mosby, St Louis, 1989.
- [3] T. Tsuka, T. Hamada, S. Yamada, *J. Prosthet. Dent.* 42 (1979) 262–270.
- [4] A.B. Carr, W.A. Brantley, *J. Prosthet. Dent.* 69 (1993) 391–397.
- [5] A.B. Carr, W.A. Brantley, *J. Prosthet. Dent.* 75 (1996) 77–85.
- [6] N. Leung, G.A. Zarb, P.A. Watson, *J. Dent. Res.* 60 (1982) 324 (Special Issue) [abstr. no. 1308].
- [7] N. Leung, G.A. Zarb, R.M. Pilliar, *J. Dent. Res.* 62 (1983) 293 (Special Issue) [abstr. no. 1112].
- [8] A.B. Carr, W.A. Brantley, *Int. J. Prosthodont.* 4 (1991) 265–275.
- [9] S.M. Cohen, A. Kakar, T.K. Vaidyanathan, T. Viswanadhan, *J. Prosthet. Dent.* 76 (1996) 125–131.
- [10] Cai Thesis 1992.
- [11] W.A. Brantley, Z. Cai, A.B. Carr, J.C. Mitchell, *Cells Mater.* 3 (1993) 103–114.
- [12] J.M. Van der Zel, M.M.A. Vrijhoef, *J. Oral Rehabil.* 15 (1988) 163–166.
- [13] T.D. Papadopoulos, P. Lagouvardos, *Hellenic Dent. J.* 2 (1992) 75–78.
- [14] D. Sun, P. Monaghan, W.A. Brantley, W.M. Johnston, *J. Prosthet. Dent.* 87 (2002) 86–93.
- [15] K.-T. Oh, K.-N. Kim, *J. Biomed. Mater. Res. Appl. Biomater.* 70B (2004) 318–331.
- [16] A.B. Carr, Z. Cai, W.A. Brantley, J.C. Mitchell, *Int. J. Prosthodont.* 6 (1993) 233–241.
- [17] T.D. Gilson, K. Asgar, F.A. Peyton, *J. Prosthet. Dent.* 15 (1965) 464–473.
- [18] D. Porter, K. Easterling, *Phase Transformations in Metals and Alloys*, second ed., Chapman & Hall, London, 1992.
- [19] M. Darabara, L. Bourithis, S. Zinelis, G. Papadimitriou, *Int. Endodont. J.* 37 (2004) 705–710.